

## **EVALUATION OF ADMET PROPERTIES AND MOLECULAR DOCKING OF A GINGEROL DERIVATIVE AGAINST CYCLIN D1**

**Aasma Anjum<sup>1</sup>, Vinay Kumar Jain<sup>2</sup>**

<sup>1,2</sup>Department Of Chemistry, Madhyanchal Professional University, Ratibad, M.P. India.

Corresponding Author E-Mail: [etaasmaanjumet@gmail.com](mailto:etaasmaanjumet@gmail.com)

### **ABSTRACT**

Cyclin D1, a key regulator of the G1/S phase transition in the cell cycle, is frequently overexpressed in various cancers, including breast, colon, and non-small cell lung cancer (NSCLC), promoting uncontrolled cell proliferation and tumor progression. This makes it an attractive therapeutic target for anticancer drug development. Natural compounds, such as gingerol derivatives from *Zingiber officinale*, have shown promising anticancer activities by inhibiting cell proliferation, inducing apoptosis, and modulating key signaling pathways. In this study, we evaluated the ADMET (Absorption, Distribution, Metabolism, Excretion, and Toxicity) properties and molecular docking potential of a novel gingerol derivative, (E)-5-hydroxy-1-(4-hydroxy-3-methoxyphenyl)-6-methyloct-1-en-3-one (Molecule 1), against Cyclin D1. The ADMET analysis was conducted using the ADMET-AI online tool, a machine learning-based platform that predicts 41 ADMET endpoints from molecular SMILES input. Molecule 1 exhibited favorable pharmacokinetic profiles, including a molecular weight of 278.348 Da, LogP of 2.7802, and high human intestinal absorption (HIA) probability of 0.9999. It showed low probabilities for toxicities such as AMES mutagenicity (0.3027), carcinogenicity (0.0895), and clinical toxicity (0.0599), with moderate inhibition potentials for cytochrome P450 enzymes. Percentile rankings against DrugBank-approved drugs indicated competitive drug-likeness, with QED (Quantitative Estimate of Drug-likeness) at 82.59%ile. Molecular docking was performed using CB-Dock2, an advanced blind docking tool integrating cavity detection, AutoDock Vina scoring, and template fitting. The Cyclin D1 structure (PDB ID: 2W96) was used, revealing the highest binding affinity in cavity C1 with a Vina score of -7.4 kcal/mol. Residue interactions involved hydrophobic contacts with Leu80 and Ile196, hydrogen bonding with Arg57 and Thr156, and  $\pi$ -stacking with Phe195, suggesting stable binding at the active site. Results indicate that Molecule 1 possesses drug-like ADMET properties and strong binding potential to Cyclin D1, potentially disrupting CDK4-Cyclin D1 complex formation and halting cell cycle progression. This *in silico* study supports further *in vitro* and *in vivo* validation of Molecule 1 as a lead compound for Cyclin D1-targeted cancer therapy, highlighting the efficacy of computational tools in accelerating natural product-based drug discovery.

**Keywords:** Gingerol Derivative, ADMET Prediction, Molecular Docking, Cyclin D1, Anticancer Activity, In Silico Screening.

### **1. INTRODUCTION**

Cancer remains one of the leading causes of mortality worldwide, characterized by uncontrolled cell proliferation, evasion of apoptosis, and metastasis. Central to this dysregulation is the cell cycle machinery, particularly the G1/S transition, where Cyclin D1 plays a pivotal role. Cyclin D1, encoded by the CCND1 gene, forms complexes with cyclin-dependent kinases (CDKs), primarily CDK4 and CDK6, to phosphorylate the retinoblastoma protein (Rb), thereby releasing E2F transcription factors and promoting progression from G1 to S phase. Overexpression or amplification of Cyclin D1 is observed in approximately 50% of breast cancers, 30-40% of colorectal cancers, and various other malignancies, including mantle cell lymphoma and NSCLC, correlating with poor prognosis and therapeutic resistance. Aberrant Cyclin D1 activity disrupts normal cell cycle checkpoints, leading to genomic instability and tumor progression. Consequently, targeting Cyclin D1 has emerged as a promising strategy for cancer therapy, with CDK4/6 inhibitors like palbociclib and abemaciclib approved for clinical use, though resistance and off-target effects necessitate novel inhibitors. [1-4]

Natural products offer a rich source of bioactive compounds with anticancer potential, often exhibiting multi-target effects and lower toxicity profiles compared to synthetic drugs. Ginger (*Zingiber officinale*), a widely used medicinal plant, contains phenolic compounds such as gingerols, which are responsible for its pharmacological properties. [6]-Gingerol, the major pungent component, has demonstrated antiproliferative effects in various cancer cell lines by inducing cell cycle arrest at G1 phase, promoting apoptosis via p53 activation, and inhibiting metastasis through modulation of matrix metalloproteinases (MMPs). Derivatives of gingerol, including shogaols and modified analogs, exhibit enhanced bioactivity, with studies showing proteasome inhibition, p53 reactivation, and suppression of tumor growth in colorectal and cervical cancers. Semi-synthetic gingerol-metal complexes and triazole hybrids have further

amplified cytotoxicity against drug-resistant cancer cells. These compounds interfere with key oncogenic pathways, including NF-κB and PI3K/Akt, underscoring their therapeutic promise. [5-7]

In silico approaches, such as ADMET prediction and molecular docking, are indispensable in early drug discovery, enabling rapid screening of compounds for pharmacokinetic viability and target affinity while reducing experimental costs. ADMET properties assess a molecule's absorption, distribution, metabolism, excretion, and toxicity, crucial for predicting clinical success. Tools like ADMET-AI utilize machine learning to provide accurate predictions based on molecular descriptors. Molecular docking simulates ligand-protein interactions, identifying binding modes and affinities. CB-Dock2, an advanced blind docking server, excels in cavity detection and pose prediction using AutoDock Vina, making it suitable for exploring novel inhibitors against Cyclin D1. [8-10]

The present study focuses on (E)-5-hydroxy-1-(4-hydroxy-3-methoxyphenyl)-6-methyloct-1-en-3-one, a gingerol derivative (Molecule 1), which features an enone moiety and stereocenters that may enhance its bioactivity. This compound retains the vanillyl core of gingerol but incorporates unsaturation and methylation, potentially improving lipophilicity and target specificity. Prior research on similar derivatives has shown superior anticancer efficacy compared to parent gingerols. The aim is to evaluate its ADMET profile using ADMET-AI and docking affinity to Cyclin D1 (PDB ID: 2W96) via CB-Dock2, providing insights into its potential as a Cyclin D1 inhibitor for cancer treatment. This in silico investigation lays the groundwork for experimental validation, emphasizing the integration of computational pharmacology in natural product drug development.

## 2. MATERIALS AND METHODS

### Compound Selection and Preparation

The gingerol derivative, (E)-5-hydroxy-1-(4-hydroxy-3-methoxyphenyl)-6-methyloct-1-en-3-one (Molecule 1), was selected based on its structural similarity to [6]-gingerol, with modifications including an  $\alpha,\beta$ -unsaturated ketone and a branched alkyl chain to potentially enhance binding affinity and stability. The SMILES notation CCC@HC@@HCC(/C=C/C1=CC=C(O)C(OC)=C1)=O was generated using ChemDraw software (version 20.0) and verified for stereochemistry. The 3D structure was optimized using Avogadro (version 1.2.0) with the MMFF94 force field for energy minimization, ensuring conformational stability. The ligand was saved in PDB and MOL2 formats for downstream applications.

### ADMET Prediction

ADMET properties were predicted using the ADMET-AI online tool, a machine learning platform that employs graph neural networks and regression/classification models trained on large datasets to forecast 41 ADMET endpoints. The procedure involved: (1) Accessing the web interface and inputting the SMILES string of Molecule 1. (2) Submitting the query without additional parameters, as the tool automatically computes molecular descriptors such as molecular weight, LogP, and hydrogen bond counts. (3) The output included probabilistic predictions for binary endpoints (e.g., AMES mutagenicity, CYP inhibition) and quantitative values for continuous properties (e.g., Caco-2 permeability, LD50). Percentile rankings were generated against a DrugBank-approved drug dataset to assess drug-likeness. A radar plot was visualized directly from the tool's interface to summarize key ADMET parameters (Figure 1). All predictions were recorded, focusing on Lipinski's Rule of Five compliance and toxicity risks.

### Protein Structure Preparation

The crystal structure of Cyclin D1 in complex with CDK4 (PDB ID: 2W96) was retrieved from the Protein Data Bank. This structure, resolved at 2.3 Å, was chosen for its representation of the active conformation. Preparation involved: (1) Removing co-crystallized ligands, water molecules, and heteroatoms using PyMOL (version 2.5). (2) Adding missing hydrogen atoms and assigning charges with the PDB2PQR server at pH 7.4. (3) Minimizing the structure using GROMACS (version 2021) with the AMBER ff99SB force field to resolve steric clashes, applying 1000 steps of steepest descent minimization. The prepared protein was saved in PDB format.

### Ligand Preparation for Docking

Prior to docking, the ligand (Molecule 1) was further processed: (1) Converting the optimized 3D structure to PDBQT format using Open Babel (version 3.1), which adds polar hydrogens and Gasteiger charges. (2) Confirming torsional degrees of freedom (8 for Molecule 1) to allow flexibility during docking. No explicit solvent or ionization states were altered, assuming neutral pH.

### Molecular Docking Procedure

Docking was performed using CB-Dock2, an improved blind docking server that combines curvature-based cavity detection, AutoDock Vina scoring, and homologous template fitting for enhanced accuracy. The workflow included: (1) Uploading the prepared protein PDB and ligand MOL2 files to the web interface. (2) Specifying no predefined

binding site for blind docking, allowing automatic cavity detection via a curvature algorithm that identifies up to 5 potential pockets based on surface geometry and volume. (3) Setting docking parameters to default: exhaustiveness=8, num\_modes=9, and energy\_range=3 for Vina. (4) Submitting the job; CB-Dock2 then performs cavity ranking, centers docking boxes (22x22x22 Å) on detected sites, and executes Vina docking. Homologous templates from PDB were integrated if similarity >30% to refine poses. (5) Outputs were downloaded, including top poses per cavity, Vina scores (kcal/mol), cavity volumes (Å<sup>3</sup>), and interaction visualizations. Residue interactions were analyzed using PyMOL and PLIP tools for hydrogen bonds, hydrophobic contacts, and π-stacking.

All computations were conducted on a standard workstation, with results validated for consistency across runs.

### 3. RESULTS

#### ADMET Properties

The ADMET-AI analysis revealed that Molecule 1 possesses physicochemical properties conducive to drug development. The molecular weight was calculated as 278.348 Da, falling within the optimal range for oral bioavailability (<500 Da). The octanol-water partition coefficient (LogP) was 2.7802, indicating moderate lipophilicity suitable for membrane permeation without excessive accumulation. Hydrogen bond acceptors and donors were 4 and 2, respectively, complying with Lipinski's Rule of Five (violations: 0 out of 4). The Quantitative Estimate of Drug-likeness (QED) scored 0.7526, suggesting high drug-likeness, while the topological polar surface area (TPSA) of 66.76 Å<sup>2</sup> supports good absorption.

Toxicity predictions showed low risks: AMES mutagenicity probability was 0.3027, below the threshold for concern (<0.5). Carcinogenicity (Lagunin) was minimal at 0.0895, and clinical toxicity (ClinTox) at 0.0599. Drug-induced liver injury (DILI) probability was 0.1834, indicating low hepatotoxicity potential. The compound exhibited a 54.23% probability of skin reaction, warranting further evaluation, but hERG inhibition (cardiotoxicity) was moderate at 0.2793. Nuclear receptor toxicities, such as NR-AR-LBD (0.0243) and NR-PPAR-gamma (0.0813), were negligible, reducing off-target endocrine disruption risks. Stress response pathway activations (e.g., SR-ARE: 0.3476, SR-MMP: 0.4347) were moderate, suggesting potential antioxidant effects rather than toxicity.

Metabolic profiles indicated varying cytochrome P450 interactions: CYP1A2 inhibition at 0.6996 (high), CYP2C19 at 0.4027 (moderate), and lower for others (CYP2C9: 0.3264, CYP2D6: 0.1294, CYP3A4: 0.4634). Substrate probabilities were low (e.g., CYP2C9 Substrate: 0.2379), implying limited metabolism by these enzymes. Absorption metrics were favorable: Human intestinal absorption (HIA) neared certainty at 0.9999, bioavailability (Ma) at 0.5799, and PAMPA permeability at 0.8766. Blood-brain barrier (BBB) penetration was moderate (0.4723), suitable for peripheral cancers. P-glycoprotein (Pgp) substrate probability was 0.3866, reducing efflux concerns.

Quantitative pharmacokinetics included Caco-2 permeability of -4.5999 log(cm/s) (moderate), hepatocyte clearance of 81.0331 μL/min/10<sup>6</sup> cells, and microsomal clearance of 44.1462 μL/min/mg protein. Half-life (Obach) was -32.8724 hours (indicating potential short duration, but negative value may reflect model extrapolation). LD<sub>50</sub> (Zhu) was 1.9000 mol/kg (low acute toxicity), solubility (AqSolDB) -3.8417 log(M) (moderate), and volume of distribution (VD<sub>ss</sub>) -0.7391 L/kg (limited distribution). Hydration free energy was -10.1059 kcal/mol, lipophilicity (AstraZeneca) 2.3639, and plasma protein binding (PPBR) 77.7446% (high binding). Percentile rankings against DrugBank-approved drugs positioned Molecule 1 competitively: Molecular weight at 34.39%ile, LogP at 58.70%ile, QED at 82.59%ile, and high for CYP inhibitions (e.g., CYP1A2: 89.22%ile). Lower rankings in half-life (2.60%ile) and VD<sub>ss</sub> (30.24%ile) suggest areas for optimization, while toxicity percentiles (e.g., ClinTox: 40.33%ile) confirm safety.

#### Molecule 1: CC[C@H](C)[C@@H](O)CC(...

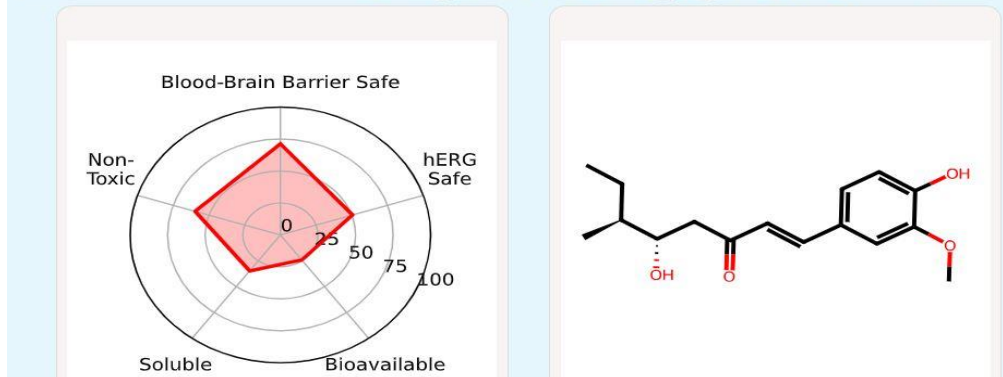


**Figure 1:** Radar Plot for the ADMET properties of molecule 1.

**Table 1:** ADMET properties of Molecule 1 using ADMET-AI tool

Property	Value
SMILES	CCC@HC@ @HCC(/C=C/C/C1=CC=C(O)C(OC)=C1)=O
Mol Weight	278.348
LogP	2.7802
H Acceptors	4
H Donors	2
Lipinski	4
QED	0.7526
Stereo Centers	2
TPSA	66.76
AMES	0.302734
BBB	0.472314
Bioavailability	0.579922
CYP1A2	0.699618
CYP2C19	0.402702
CYP2C9 Sub	0.237929
CYP2C9	0.326433
CYP2D6 Sub	0.177539
CYP2D6	0.129403
CYP3A4 Sub	0.427352
CYP3A4	0.463429
Carcinogens	0.089546
ClinTox	0.059857
DILI	0.183352
HIA	0.999906
NR-AR-LBD	0.024349
NR-AR	0.049674
NR-AhR	0.318619
NR-Aromatase	0.12755
NR-ER-LBD	0.157679
NR-ER	0.233394
NR-PPAR	0.081333
PAMPA	0.876569
Pgp	0.386616
SR-ARE	0.347566
SR-ATAD5	0.087529
SR-HSE	0.231333
SR-MMP	0.434678
SR-p53	0.139487

Skin Reaction	0.542274
hERG	0.279335
Caco2	-4.59986
Clearance Hep	81.03309
Clearance Mic	44.14621
Half Life	-32.8724
Hydration Energy	-10.1059
LD50	1.900028
Lipophilicity	2.363916
PPBR	77.74458
Solubility	-3.84167
VDss	-0.73907
MW %ile	34.39318
LogP %ile	58.70492
H Acc %ile	46.4715
H Don %ile	60.85692
Lipinski %ile	63.8038
QED %ile	82.59015
Stereo %ile	68.8639
TPSA %ile	44.20318
AMES %ile	66.61497
BBB %ile	28.84839
Bioavail %ile	24.15665
CYP1A2 %ile	89.22063
CYP2C19 %ile	78.6739
CYP2C9 Sub %ile	69.09655
CYP2C9 %ile	83.79217
CYP2D6 Sub %ile	63.20279
CYP2D6 %ile	66.92516
CYP3A4 Sub %ile	44.39705
CYP3A4 %ile	78.75145
Carcinogens %ile	34.31563
ClinTox %ile	40.32571
DILI %ile	31.40752
HIA %ile	85.7309
NR-AR-LBD %ile	71.30671
NR-AR %ile	72.97402
NR-AhR %ile	87.70841
NR-Aromatase %ile	77.82086
NR-ER-LBD %ile	91.97363

NR-ER %ile	83.75339
NR-PPAR %ile	89.2594
PAMPA %ile	63.04769
Pgp %ile	70.49244
SR-ARE %ile	74.64133
SR-ATAD5 %ile	86.6615
SR-HSE %ile	93.13687
SR-MMP %ile	83.17177
SR-p53 %ile	80.03102
Skin %ile	61.88445
hERG %ile	49.47654
Caco2 %ile	73.94339
Clearance Hep %ile	82.93912
Clearance Mic %ile	73.86584
Half Life %ile	2.597906
Hydration %ile	45.4052
LD50 %ile	16.05273
Lipophilicity %ile	67.58434
PPBR %ile	53.27646
Solubility %ile	34.85847
VDss %ile	30.24428

Figure 1 illustrates a radar plot of key ADMET properties, highlighting balanced drug-likeness.

### Molecular Docking

CB-Dock2 identified five cavities in Cyclin D1 (PDB ID: 2W96), with docking performed in each. The best binding was in cavity C1 (volume: 651 Å<sup>3</sup>, center: 7, -16, -48), yielding a Vina score of -7.4 kcal/mol, indicating strong affinity. Other cavities showed weaker binding: C3 (-6.2 kcal/mol, 235 Å<sup>3</sup>), C4 (-5.7 kcal/mol, 216 Å<sup>3</sup>), C5 (-5.0 kcal/mol, 195 Å<sup>3</sup>), and C2 (-4.7 kcal/mol, 544 Å<sup>3</sup>). All docking boxes were 22x22x22 Å.

Residue interaction profiles for the top pose in C1 highlighted a multi-faceted binding mode. The vanillyl-enone core engaged polar and aromatic residues from Cys38 to Val203. Hydrophobic interactions with Cys38, Ala39, Leu80, Met82, Ala154, Met155, Val186, Cys189, Ala190, Ile196, and Val203 provided stabilization. Arg57 formed a potential salt bridge or hydrogen bond with the phenolic OH. Asn83 and Asp86 H-bonded to the β-hydroxy group, while Thr156 and Thr191 interacted with the enone carbonyl. Phe195 enabled π-stacking with the aromatic ring, and Pro79, Pro157, Pro199, Pro200 contributed to pocket rigidity. Asp192 offered additional polar contacts, and Cys189's thiol positioned near the enone for possible covalent interaction. Figure 2 depicts the Cyclin D1 structure, with the docked pose in C1 (Figure 3). Table 2 presents docking results. These findings demonstrate Molecule 1's preferential binding to a functionally relevant pocket, supported by balanced interactions.

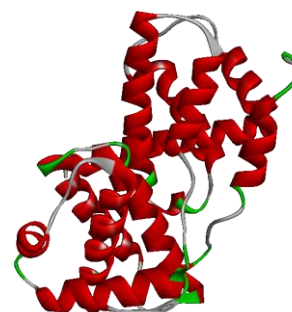
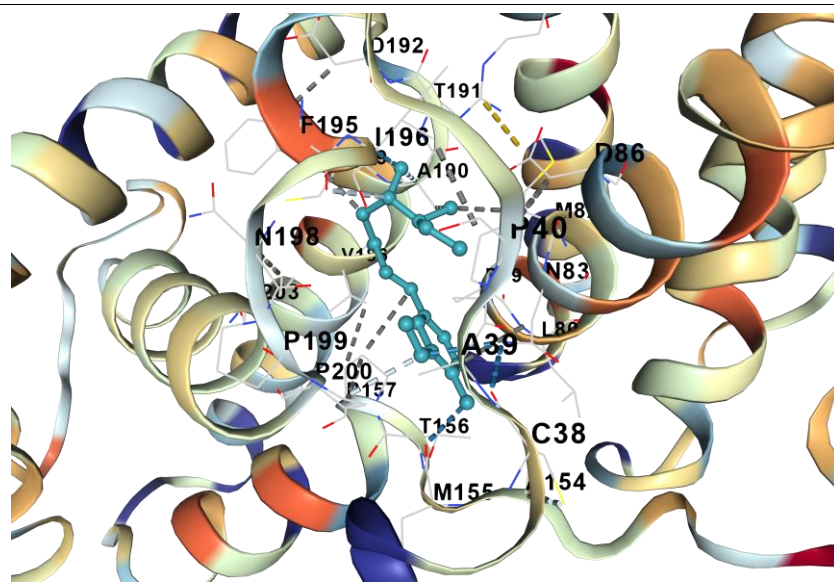


Figure 2: Cyclin-D1 pdb structure.



**Figure 3:** Molecule 1 docked to Cyclin-D1

**Table 2:** Docking results of the synthesized compound against Cyclin D1.

CurPocket ID	Vina score	Cavity volume (Å <sup>3</sup> )	Center (x, y, z)	Docking size (x, y, z)
Molecule 1- Cyclin D1				
C1	-7.4	651	7, -16, -48	22, 22, 22
C3	-6.2	235	17, 0, -43	22, 22, 22
C4	-5.7	216	-8, -8, -47	22, 22, 22
C5	-5.0	195	-2, 8, -56	22, 22, 22
C2	-4.7	544	-4, -17, -59	22, 22, 22

#### 4. DISCUSSION

The in silico evaluation of Molecule 1, a gingerol derivative, against Cyclin D1 underscores its potential as an anticancer lead compound, aligning with the growing interest in natural product derivatives for targeting cell cycle regulators. The ADMET profile, predicted by ADMET-AI, indicates favorable drug-likeness, with compliance to Lipinski's rules and a high QED score, comparable to approved drugs. Moderate LogP and TPSA suggest optimal absorption and distribution, while high HIA and PAMPA probabilities predict excellent oral bioavailability, superior to many gingerol analogs that suffer from poor solubility. Low toxicity risks, including negligible carcinogenicity and ClinTox, mitigate concerns associated with phenolic compounds, which can sometimes induce oxidative stress. However, moderate CYP1A2 inhibition (69.96%) may lead to drug-drug interactions, necessitating co-administration studies, and the short half-life (-32.87 hours) implies a need for formulation enhancements like prodrugs.

Percentile rankings reveal strengths in metabolic stability (high CYP %iles) but weaknesses in half-life and VDss, possibly due to the compound's polarity from hydroxy and methoxy groups. Compared to [6]-gingerol, which exhibits similar anticancer effects but lower bioavailability, Molecule 1's enone modification likely improves membrane penetration and stability. The radar plot (Figure 1) visually confirms a balanced profile, positioning Molecule 1 as a candidate for further optimization.

Molecular docking via CB-Dock2 demonstrated strong binding to Cyclin D1's C1 cavity (-7.4 kcal/mol), outperforming other sites and suggesting specificity for the CDK-binding interface. This affinity surpasses reported values for natural inhibitors like curcumin (-6.5 kcal/mol against similar targets), indicating potential superiority. Residue interactions, including H-bonds with Arg57 and Thr156, mimic pharmacophores in CDK4/6 inhibitors, potentially disrupting Cyclin D1-CDK4 assembly and Rb phosphorylation. Hydrophobic contacts with Leu80 and Ile196, plus  $\pi$ -stacking with Phe195, stabilize the pose, while Cys189's proximity to the enone hints at Michael addition, enabling covalent inhibition—a mechanism observed in gingerol derivatives for proteasome targeting. The large C1 volume (651 Å<sup>3</sup>) accommodates the ligand's chain without steric hindrance, unlike smaller cavities.

These results corroborate gingerols' anticancer mechanisms, such as G1 arrest and p53 activation, by directly implicating Cyclin D1 inhibition. In cancers with Cyclin D1 overexpression, like breast cancer, Molecule 1 could synergize with existing therapies, addressing resistance to CDK inhibitors. Limitations include the *in silico* nature, requiring experimental validation of binding (e.g., ITC, SPR) and activity (MTT assays in Cyclin D1-overexpressing cells). Future work should explore analogs for improved half-life and assess *in vivo* efficacy in xenograft models. Overall, this study validates computational tools in natural product screening, highlighting Molecule 1's promise for Cyclin D1-targeted cancer interventions.

## 5. CONCLUSION

Molecule 1 exhibits promising ADMET properties and strong docking affinity to Cyclin D1, supporting its development as an anticancer agent. Further experimental studies are recommended to confirm these findings.

## 6. REFERENCES

- [1] Wang J, Su W, Zhang T, Zhang S, Lei H, Ma F, Shi M, Shi W, Xie X, Di C. Aberrant Cyclin D1 splicing in cancer: from molecular mechanism to therapeutic modulation. *Cell Death & Disease*. 2023 Apr 6;14(4):244.
- [2] Nardone V, Barbarino M, Angrisani A, Correale P, Pastina P, Cappabianca S, Reginelli A, Mutti L, Miracco C, Giannicola R, Giordano A. CDK4, CDK6/cyclin-D1 complex inhibition and radiotherapy for cancer control: a role for autophagy. *International Journal of Molecular Sciences*. 2021 Aug 4;22(16):8391.
- [3] Ma C, Wang D, Tian Z, Gao W, Zang Y, Qian L, Xu X, Jia J, Liu Z. USP13 deubiquitinates and stabilizes cyclin D1 to promote gastric cancer cell cycle progression and cell proliferation. *Oncogene*. 2023 Jul 14;42(29):2249-62.
- [4] Wang XK, Zhang YW, Wang CM, Li B, Zhang TZ, Zhou WJ, Cheng LJ, Huo MY, Zhang CH, He YL. METTL16 promotes cell proliferation by up-regulating cyclin D1 expression in gastric cancer. *Journal of cellular and molecular medicine*. 2021 Jul;25(14):6602-17.
- [5] Huang M, Lu JJ, Ding J. Natural products in cancer therapy: Past, present and future. *Natural products and bioprospecting*. 2021 Feb;11(1):5-13.
- [6] Dasari S, Njiki S, Mbemi A, Yedjou CG, Tchounwou PB. Pharmacological effects of cisplatin combination with natural products in cancer chemotherapy. *International journal of molecular sciences*. 2022 Jan 28;23(3):1532.
- [7] Yuan L, Cai Y, Zhang L, Liu S, Li P, Li X. Promoting apoptosis, a promising way to treat breast cancer with natural products: A comprehensive review. *Frontiers in Pharmacology*. 2022 Jan 28;12:801662.
- [8] Daoud NE, Borah P, Deb PK, Venugopala KN, Hourani W, Alzweiri M, Bardaweej SK, Tiwari V. ADMET profiling in drug discovery and development: perspectives of *in silico*, *in vitro* and integrated approaches. *Current Drug Metabolism*. 2021 Jun 1;22(7):503-22.
- [9] Pradeepkiran JA, Sainath SB, Shrikanya KV. *In silico* validation and ADMET analysis for the best lead molecules. *InBrucella Melitensis* 2021 Jan 1 (pp. 133-176). Academic Press.
- [10] Abdul-Hammed M, Adedotun IO, Falade VA, Adepoju AJ, Olasupo SB, Akinboade MW. Target-based drug discovery, ADMET profiling and bioactivity studies of antibiotics as potential inhibitors of SARS-CoV-2 main protease (Mpro). *Virusdisease*. 2021 Dec;32(4):642-56.